Journal of ELECTRONIC MATERIALS, Vol. 40, No. 8, 2011
DOI: 10.1007/s11664-011-1648-3

Microstructure of Heteroepitaxial ZnTe Grown by Molecular Beam Epitaxy on Si(211) Substrates

X.J. WANG,[1,3] Y. CHANG,[1] C.R. BECKER,[1] C.H. GREIN,[1] S. SIVANANTHAN,[1] and R. KODAMA[2]

1.—Microphysics Laboratory, Department of Physics, University of Illinois at Chicago, Chicago, IL 60607, USA. 2.—EPIR Technologies Inc., Chicago, IL 60607, USA. 3.—e-mail: xwang31@uic.edu

The interface of ZnTe/Si(211) grown by molecular beam epitaxy was investigated by high-resolution transmission electron microscopy. Several types of defects such as misfit dislocations, stacking faults, agglomerations of vacancies, and precipitates were observed and studied by electron microscopy at the ZnTe/Si interface. The distribution of misfit dislocations at the interface was revealed with the assistance of the fast Fourier transformation filtering technique. A stick-and-ball interface model including misfit dislocation geometry is proposed. The possible origins of the stacking faults, vacancies, and precipitates are discussed.

Key words: ZnTe, Si, dislocations, molecular beam epitaxy

INTRODUCTION

CdTe(211)B/Si(211) is of great current interest as an alternative substrate for large-area epitaxial HgCdTe growth. In spite of the 19.3% lattice mismatch between CdTe and Si, good-quality CdTe can be grown on Si(211). Acceptable crystal quality and electrical characteristics of HgCdTe grown on CdTe(211)B/Si(211) by molecular beam epitaxy (MBE) have been demonstrated.[1] Furthermore, MBE-grown CdTe on Si has proven to be a promising heterostructure for high-efficiency solar cells, which can greatly lower the cost per watt of single- and multijunction solar cells.[2] It is essential to grow ZnTe on As-passivated Si(211) substrates before deposition of CdTe to alleviate the significant lattice mismatch between CdTe and Si, maintain the (211) orientation for the subsequent CdTe growth, and ensure that the surface is terminated with Te (B surface). In addition, it has been demonstrated that thin ZnTe films with about 1 μm thickness can also function very well as a buffer layer for PbSe growth by MBE, because the lattice constant of ZnTe is close to that of PbSe[3] (the lattice mismatch of the two materials is only 0.3% at room temperature).

(Received December 17, 2010; accepted April 5, 2011; published online May 3, 2011)

Numerous studies have been carried out in recent decades on this important ZnTe(211)/Si(211) interface to understand the nucleation process and growth mode.[4–7] The Si(211) surface provides a periodic step array which is composed of terraces formed by (111) crystal planes and step edges formed by (100) crystal planes, making angles of 19.47° and 35.25°, respectively. There are two silicon atoms on one terrace, each with one dangling bond, while each step edge is occupied by only one silicon atom with two dangling bonds. Therefore, the step edge has a greater chance to bond with impinging atoms during growth. The Si(211) surface thus provides a distinctive template in which energetically favorable nucleation sites (step edges) are arranged periodically. As a result, regular and uniform initial nucleation is promoted and a highly ordered thin film with low dislocation density is produced. However, uniform initial nucleation of adatoms on a silicon substrate cannot be ensured by the (211)-oriented surface alone. Because the binding energy between Te and Si is very strong,[8] the surface potential barriers are so high that incoming atoms and molecules (Zn, Te_2, and Cd) stick to any available site on the silicon surface once they arrive at the surface, leading to randomly distributed nuclei. Later on, coalescence of islands grown from these nuclei leads to a layer with columnar-like

surface morphology containing a high density of twins and other defects. It has been determined that As-passivated silicon surface can significantly enhance the diffusion length of Te and promote initial nucleation of Te at step edges.[6,7] Arsenic adatoms are believed to replace silicon atoms at terraces formed by (111) crystal planes, leaving silicon atoms with two dangling bonds at step edges during exposure of As_4 flux to the Si(211) surface.[9] When Te_2 flux impinges on the As-passivated Si(211) surface, Te adatoms migrate on the terraces occupied by As atoms and bond with silicon atoms at the step edges preferentially because of their enhanced surface diffusion length due to the presence of the As atoms. Afterwards, Zn adatoms bond with Te and As atoms and step-flow growth starts along terraces during migration-enhanced epitaxy with alternating exposure to Te_2 and Zn fluxes.

The lattice mismatch between ZnTe and silicon is as large as 12.4% at room temperature. Consequently, defects originating from lattice mismatch cannot be ignored. These defects in the buffer layer would affect the quality of the active layer above. Furthermore, ZnTe is also a device layer in recent solar cells based on II–VI semiconductors.[2,10] Knowledge of defects and interface structure is therefore essential for improving device performance. This paper analyzes the interface structure between ZnTe and the Si(211) substrate and discusses the origin of the formation of defects near the interface using high-resolution transmission electron microscopy (HRTEM).

EXPERIMENTAL PROCEDURES

ZnTe deposition was carried out in a Riber compact 21 MBE system. Si(211) substrates were prepared by a modified Radio Corporation of America (RCA) processing method which is described elsewhere.[11] High-purity (7 N) sources of ZnTe, As, Zn, and Te were used either for ZnTe film deposition or to produce an initial nucleation layer. Reflection high-energy electron diffraction was used to *in situ* monitor the surface morphology and growth conditions. The ZnTe growth proceeds from deoxidization of the Si(211) surface by heating the substrate up to about 850°C, followed by cooling to the growth temperature under an As_4 flux to passivate the silicon surface. The initial ZnTe nucleation layer up to 20 nm thick is generated by the method of migration-enhanced epitaxy in which Te_2 flux and Zn flux are exposed to the surface alternately and the sample is annealed without flux in the intervals between flux exposures. A 1-μm-thick ZnTe thin film was then grown by means of a ZnTe compound cell. The as-grown sample was characterized by x-ray diffraction measurement; the full-width at half-maximum of the ZnTe (422) rocking curve was about 220 arcsec for the sample investigated in this investigation.

Electron microscopy samples were prepared with cross-sectional geometry. Two small pieces of the sample were glued together with adjoining ZnTe surfaces to provide multiple electron transparency areas at the interface and provide protection of the ZnTe thin film. This step was followed by polishing and dimpling of two edges of this "sandwich" to thickness of about 15 μm to 25 μm. It is important to ensure that the polishing direction is along $[0\bar{1}1]$ so that the sample along the low-index $[0\bar{1}1]$ zone axis is observed; otherwise, only lattice fringes can be displayed from other zone axes that result in projection of crystal planes that have lattice spacings beyond the practical resolution of the electron microscope used in this study. Argon-ion milling was applied as the last thinning step, in which argon beams from two guns bombarded the sample at 4 kV and 4 mA with an angle of 15° with respect to the sample surface. Low voltage (3 kV), low current (3 mA), and small milling angle (8°) were then used for 30 min to remove the amorphous layers on the sample surface. It is necessary to keep the sample at liquid-nitrogen temperature to minimize ion-milling damage. The specimen was characterized using a JEOL 3010 high-resolution transmission electron microscope, operated at 300 keV and equipped with a double-tilt, side-entry-type specimen holder. Selected-area electron diffraction (SAED) patterns were used to establish the orientation relationship between the thin ZnTe film and silicon substrate.

RESULTS AND DISCUSSION

High-index surfaces such as the (211) surface of silicon are not atomically flat due to the existence of periodic steps formed by step edges and terraces. This feature can be observed in HRTEM images with sufficiently high magnification, as shown in Fig. 1 where the "saw teeth" at the interface actually result from the periodic steps at the Si(211) surface. The angles between terraces and interface are 19.4°, suggesting that the terraces are formed by (111) crystal planes. A selective-area diffraction pattern of the interface between ZnTe and silicon is shown in the inset to Fig. 1. All of the diffraction spots except for the central undiffracted spot appear as pairs. The inner spot of each pair, closer to the central transmitted beam spot, is due to ZnTe because of its larger lattice constant, while the other diffraction spots are due to silicon. The diffracted spots correspond to specific crystalline plane, as labeled in the figure. It was determined from the alignment of the two $(\bar{4}\bar{2}\bar{2})$ diffracted spots with the central spot that ZnTe is tilted about 2.66° from substrate normal. This tilt angle was confirmed by x-ray diffraction measurements. It is very likely that this tilt angle is due to the distribution of misfit dislocations and the elastic strain caused by the presence of steps at the interface.

When ZnTe is grown on a silicon substrate, it is expected to experience large elastic strain due to the significant difference between the lattice constants of the two materials. A high density of misfit dislo-

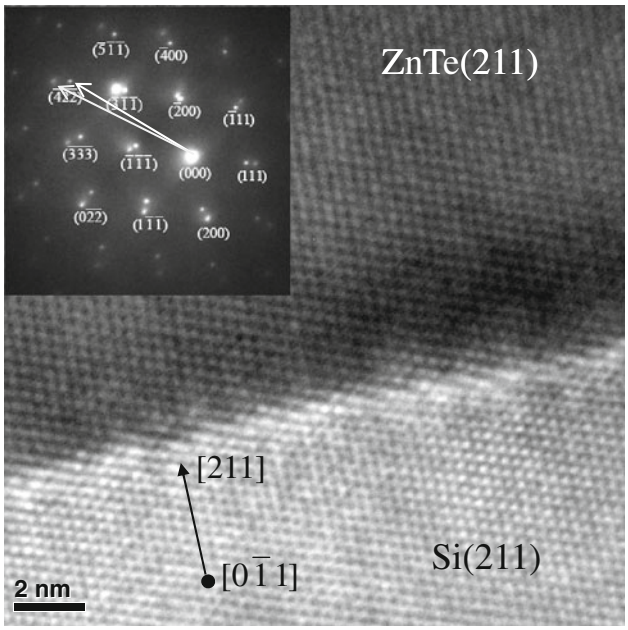

Fig. 1. High-resolution transmission electron microscopy image of the interface between ZnTe and Si(211); the inset shows a selective-area electron diffraction pattern taken from the interface.

cations is usually generated to accommodate the strain at the interface. Figure 2a shows a HRTEM image of the ZnTe/Si interface. The inset to Fig. 2a shows a magnification of the area at the interface marked by a black square. A Burgers circuit is drawn in the inset, showing that the Burgers vector is on a (111) plane and that its magnitude is the distance between two adjacent atomic sites on (111) planes. This characteristic of the Burgers vector suggests that the misfit dislocation is a perfect dislocation in which its Burgers vector is the shortest lattice translation vector $(1/2\langle 110\rangle$ in a face-centered cubic structure including zincblende structure) in the slip plane.[12]

The fast Fourier transformation (FFT) technique was used to filter Fig. 2a to highlight particular crystalline planes and misfit dislocations. The FFT produces a diffractogram of the HRTEM image in frequency space. The frequency space of a crystal is merely the reciprocal space which can be mapped by a diffraction pattern. The next step is to apply mask(s) to the diffractogram to select particular frequencies, which are represented by bright spot(s). Masks are created by using masking tools which are twin ovals in Gatan Digital Micrograph™ 1.70.16. Once masks are applied, the last step is to inverse Fourier transform the diffractogram to real space to show the filtered image originating from the bright spots in the diffractogram. Figure 2b, c, and d show filtered images of Fig. 2a which only display the area around the interface and show $(\bar{1}11)$, (100), and (111) crystal planes, respectively. The misfit dislocations identified by the location of the ends of extra half-planes are marked by red

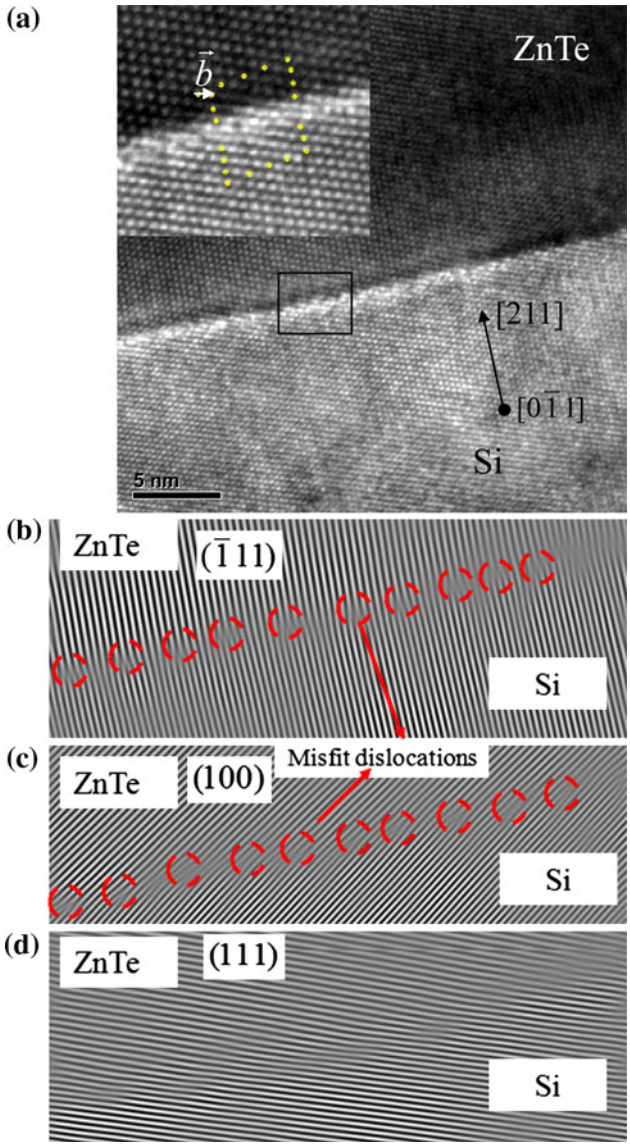

Fig. 2. (a) High-resolution TEM image of the ZnTe and Si(211) interface; the inset shows a magnified image of a particular area of the interface marked by a black square. (b) Inverse fast Fourier transformation image showing only $(\bar{1}11)$ crystalline planes. (c) Inverse fast Fourier transformation image showing only (100) crystalline planes. (d) Inverse fast Fourier transformation image showing only (111) crystalline planes.

circles. It was found that a dislocation array appears at the interface on $(\bar{1}11)$ and (100) planes, but, in contrast, there are no misfit dislocations on the (111) planes. In other words, (111) planes are aligned across the interface in spite of the existence of a 12.4% lattice mismatch. This phenomenon is in agreement with the fact that the Burgers vector in this system is on the (111) crystalline plane, and it can be attributed to step flow growth along the (111) terraces. These misfit dislocations at the interface can relax the strain due to lattice mismatch. The strain remaining after relaxation can be estimated from the distribution of misfit dislocations. The

biaxial compressive strain in ZnTe thin film before relaxation can be obtained as

$$\varepsilon_{\parallel} = (a_{\parallel} - a_0)/a_0, \tag{1}$$

where a_0 is the unstrained lattice constant of ZnTe and $a_{\parallel}$ is the strained lattice constant. In the case of a pseudomorphic strained layer, $a_{\parallel}$ would be equivalent to the lattice constant of silicon. Therefore, $\varepsilon_{\parallel}$ is equal to -12.4%. The array of misfit dislocations reduces the elastic strain by

$$\delta = \vec{b} \cdot \hat{e}\langle \bar{1}11 \rangle / d, \tag{2}$$

which is the ratio between the effective Burgers vector and the average distance between two adjacent misfit dislocations, which can be determined from the inverse FFT image (Fig. 2b, c) to be 29.1 Å. In Eq. (2), $\vec{b}$ is the Burgers vector of the misfit dislocation, $\hat{e}\langle \bar{1}11 \rangle$ is the unit vector in $\langle \bar{1}11 \rangle$ direction, and $\vec{b} \cdot \hat{e}\langle \bar{1}11 \rangle$ is the projection of the Burgers vector onto the interface which actually relaxes the elastic strain.

$$\vec{b} \cdot \hat{e}\langle \bar{1}11 \rangle = 3.7 \text{ A} \times \cos(19.4^{\circ}), \tag{3}$$

where 19.4° is the theoretical angle between (111) and (211) planes.

$$\varepsilon_r = f + \delta = -0.4\%. \tag{4}$$

This implies that most of elastic strain is relaxed by the perfect dislocation array at the interface.

A stick-and-ball model showing the geometry of misfit dislocations at the ZnTe/Si interface is illustrated in Fig. 3. This model accounts for the lattice constants of ZnTe and Si, and agrees with previous conclusions about this interface and the distribution of dislocations mentioned above. The atomic sites on terraces of the Si(211) substrate are occupied by As atoms denoted by yellow circles, leaving step edges where Si atoms are present. All of the Si atoms at the step edges are bonded with Te atoms. Zn atoms bond with As atoms at the terraces. The dislocation cores always occur at the terraces, leaving one As atom with two dangling bonds inside each dislocation core, because all of the Si atoms at the step edges have bonded with Te atoms during the first exposure to the Te_2 flux. Since Zn atoms bond with As atoms at the terraces, a Te-terminated ZnTe(211) surface is ensured, which leads to the CdTe(211)B surface. Therefore, the dislocation core geometry is asymmetric in nature and can be described as an eightfold ring where an arsenic atom at the terrace has one dangling bond. By carefully checking the crystal plane alignment, (111) plane alignment across the interface is found to be very good, whereas there are extra half-planes present in the (100) and ($\bar{1}11$) planes. This agrees well with HRTEM observations.

The stacking fault is another common type of defect in CdTe/ZnTe grown on silicon substrates. In most cases, stacking faults originate at the interface and propagate into the epilayer, unlike misfit dislocations whose crystalline imperfections are restricted to the interface. Thus, understanding of stacking fault formation mechanism is an important issue in avoiding them and hence improving ZnTe and subsequent CdTe crystal quality. When ZnTe is grown on Si(211), two kinds of stacking faults usually form at the interface. One propagates in the (111) crystal plane which is inclined to the interface at an angle of 19.4°, while the other one extends its area of imperfection in a direction perpendicular to the interface. Figure 4 shows the morphology of the first type of stacking fault that originates from the interface and propagates into the thin ZnTe film in (111) crystal planes, but only for a short distance of about 10 nm from the interface. The formation of this kind of stacking fault can be attributed to the formation of Shockley partial dislocations which are produced by slip in (111) slip planes of the zincblende structure at the interface, because the imperfect area at the stacking fault shown in Fig. 4 can be visualized as a relative separation between two adjacent (111) planes at the boundary of the stacking fault. Face-centered cubic (fcc) crystals, which include the zincblende structure, can be imagined as a repeated stack of three different, closely packed (111) planes represented by A, B,

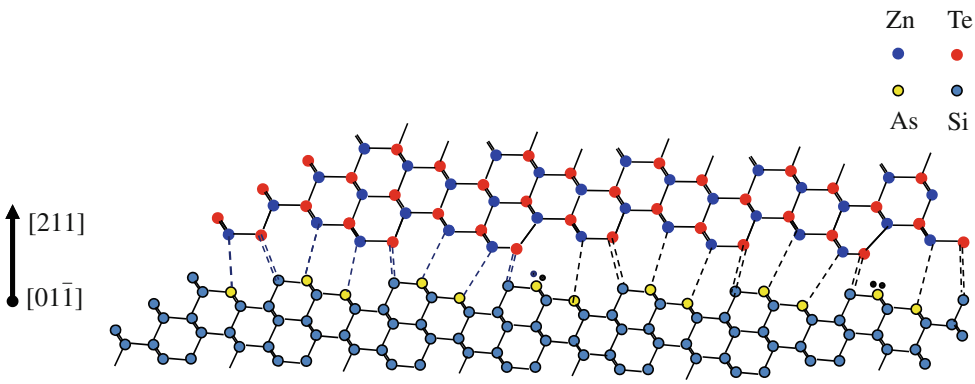

Fig. 3. Stick-and-ball model illustrating the formation of misfit dislocations at the ZnTe/Si(211) interface.

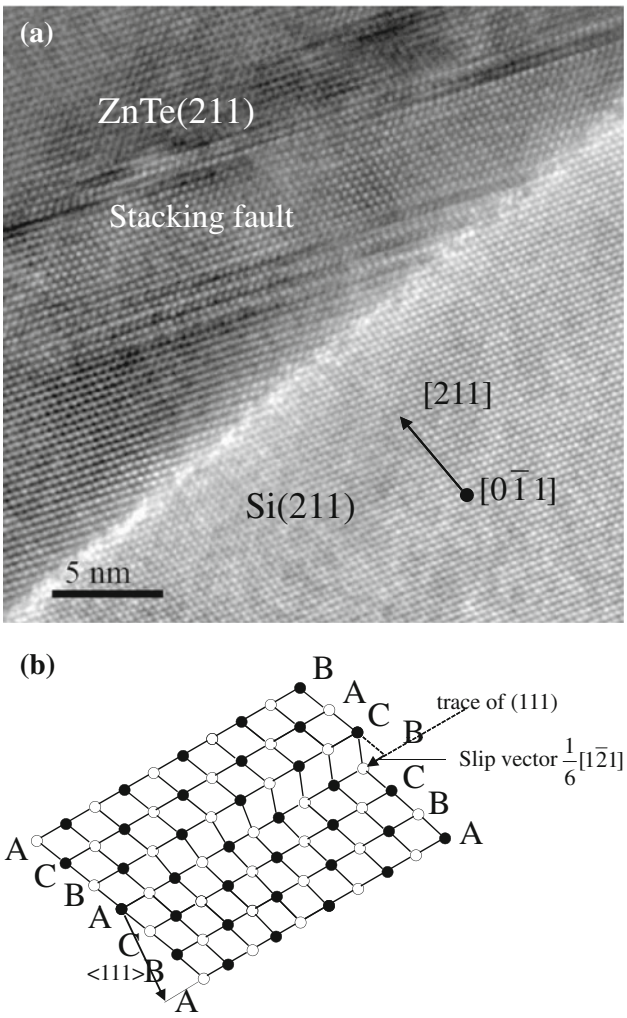

Fig. 4. (a) HRTEM image of the ZnTe/Si(211) interface showing stacking faults; (b) schematic of the formation of a Shockley partial dislocation.

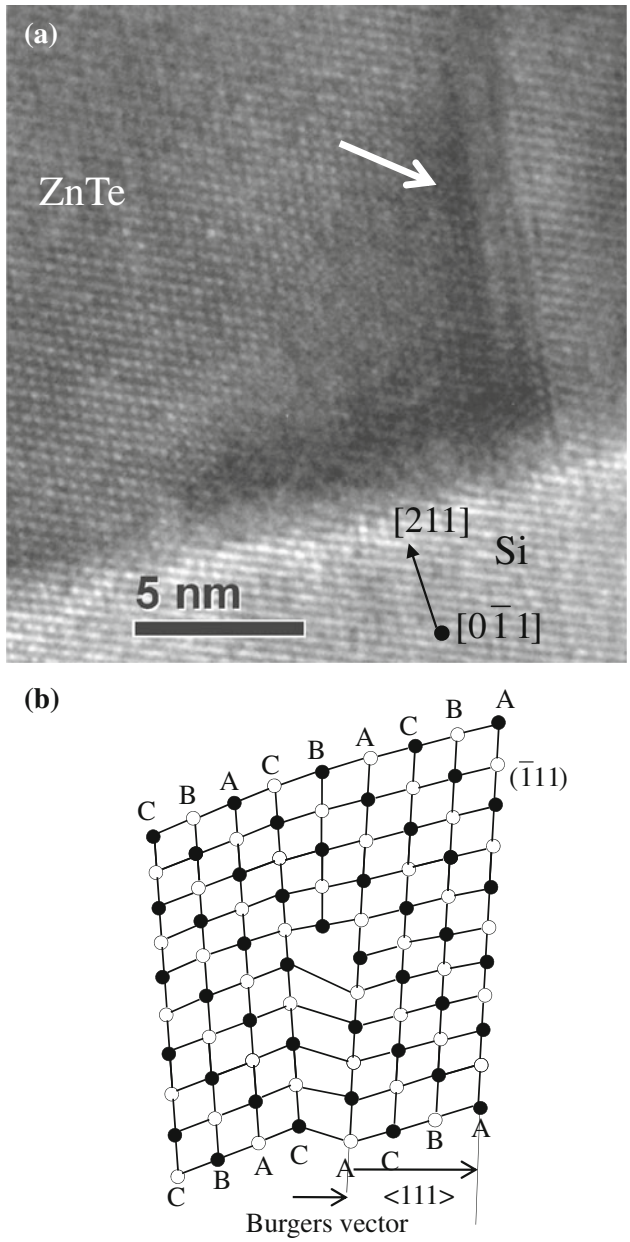

Fig. 5. (a) HRTEM image of the ZnTe/Si(211) interface showing stacking faults; (b) schematic of the formation of a Frank partial dislocation.

and C, respectively. The stacking sequence is ABCABC… in a perfect crystal. However, if the atom at position A slips to B, as shown in Fig. 4b, a stacking fault is produced. The Burgers vector of a Shockley partial dislocation is on {111} with direction of ⟨112⟩ and magnitude of $a/\sqrt{6}$, which is less than that of a perfect dislocation, i.e., $a/\sqrt{2}$.[12] Consequently, a Shockley partial dislocation as well as the associated stacking fault are caused by accommodation of the elastic misfit strain due to lattice mismatch, and strain is relaxed with less efficiency due to the shorter Burgers vector. Furthermore, it is more detrimental to the quality of crystal because the imperfect area extends into the epilayer instead of being restricted to the interface.

Another kind of stacking fault that propagates vertically into ZnTe epilayer is shown in Fig. 5. It has been observed by transmission electron microscopy in previous research.[13,14] However, its origin has not been discussed yet. The morphology of this stacking fault is due to the relative displacement of two adjacent $(\bar{1}11)$ crystal planes,[13,14] which belong to the {111} slip plane group of the zincblende structure and are perpendicular to the surface of the Si(211) substrate, at the boundary of the stacking fault. The origin of this kind of stacking fault can be attributed to the formation of a Frank partial dislocation at the interface. The Frank partial dislocation is formed by inserting or removing one closely packed {111} layer of atoms. Its Burgers vector is usually along the ⟨111⟩ direction on the crystal plane perpendicular to the slip plane ({111} plane in zincblende structure) with magnitude of $a/\sqrt{3}$ and consequently less than that of a perfect dislocation.

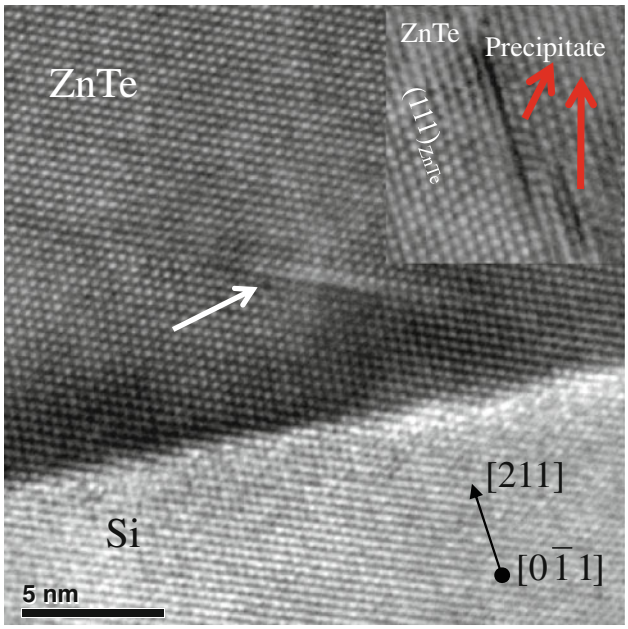

Fig. 6. HRTEM image of the ZnTe/Si(211) interface showing defects formed by collapsed vacancies; the inset shows a HRTEM image of the microstructure of Te_2 precipitates.

Specifically, at the interface between ZnTe and Si, the Frank partial dislocation is generated by removing one $(\bar{1}11)$ layer of atoms to relax the compressive strain, as shown in Fig. 5b. This Frank partial is an edge dislocation and cannot glide under the action of applied stress since it does not lie on the slip plane, unlike Shockley partial dislocations that can glide.

In summary, both kinds of stacking faults arise from the formation of partial dislocations, Shockley partial dislocations, and Frank partial dislocations. Both can alleviate misfit strain, but neither is required for strain relaxation due to the presence of a perfect misfit dislocation array as discussed previously. It is believed that the presence of stacking faults is related to growth conditions such as substrate temperature and substrate preparation. It has been noted that deviation from optimum substrate temperature could increase the density and length of stacking faults (Chang, private communication). The condition for occurrence of these two stacking faults deserves further investigation.

Vacancies and precipitates are other types of defects in ZnTe. The defect shown in Fig. 6 is on the (111) plane. The morphology of the defect shown in Fig. 6 is different from previous stacking faults. It does not originate from the interface, since the region around this defect is perfectly crystalline. It should not arise from strain relaxation, because misfit strain has been fully relaxed by a perfect dislocation array at the interface and stacking faults originating at the interface. By careful investigation of this defect, it was found that the spacings between two adjacent atoms on (111) planes were less than those at two ends of this defect as well as in a perfect area. Consequently, this defect may be produced by collapse of a platelet of vacancies. It is likely that these vacancies form in the period of annealing without flux during migration-enhanced epitaxy.

Precipitation of Te has long been a major issue in the growth of CdTe and CdZnTe single crystals.[15–17] The inset to Fig. 6 shows a high-resolution transmission electron micrograph of the microstructure of two Te precipitates located about 10 nm above the interface, as identified by a comparison of its lattice spacings with those of the adjacent ZnTe atom layers. The plane of the precipitate is collinear with $(111)_{ZnTe}$. No missing or extra planes are observed. The presence of Te precipitates may result from low-temperature growth of ZnTe [usually at 220°C, which is 80°C lower than the optimum growth temperature of ZnTe to ensure (211) orientation] which causes undissociated Te dimers.

CONCLUSIONS

High-resolution transmission electron microscopy has been used to investigate the microstructure of several types of defects in ZnTe grown on Si(211) substrates by molecular beam epitaxy. These defects include misfit dislocations, stacking faults, vacancies, and precipitates. A nearly periodic array of perfect dislocations at the interface is revealed and highlighted in HRTEM images with the assistance of FFT filtering. Most misfit strain can be relaxed by this array. Based on TEM observations and previous research, we propose that the dislocation core geometry is asymmetric in nature and can be described by eight-sided rings. Arsenic atoms at terraces with two dangling bonds each are present inside the dislocation cores. Two types of stacking faults, one propagating along (111) plane which is inclined to the interface and the other propagating vertically, are attributed to the formation of Shockley and Frank partial dislocations, respectively, at the interface due to misfit strain. Vacancies and precipitates are observed near the interfaces in HRTEM images. It is believed that these defects arise from nonstoichiometric growth during migration-enhanced epitaxy.

ACKNOWLEDGEMENTS

We acknowledge the use of the electron microscopy facilities of the Research Resource Center East at the University of Illinois at Chicago.

REFERENCES

1. M.F. Vilela, S.F. Harris, R.E. Kvaas, A.A. Buell, M.D. Newton, K.R. Olsson, D.D. Lofgreen, and S.M. Johnson, *J. Electron. Mater.* 38, 1755 (2009).
2. D. Xu, T. Biegala, M. Carmody, J.W. Garland, C. Grein, and S. Sivananthan, *Appl. Phys. Lett.* 96, 073508 (2010).
3. X.J. Wang, Y.B. Hou, Y. Chang, C.R. Becker, R.F. Klie, R. Kodama, F. Aqariden, and S. Sivananthan, *J. Cryst. Growth* 312, 910 (2010).

4. M. Jaime-Vasquez, M. Martinka, R.N. Jacobs, and J.D. Benson, *J. Electron. Mater.* 36, 905 (2007).
5. M. Jaime-Vasquez, M. Martinka, R.N. Jacobs, and M. Groenert, *J. Electron. Mater.* 35, 1455 (2006).
6. G. Brill, Y. Chen, N.K. Dhar, and R. Singh, *J. Electron. Mater.* 32, 717 (2003).
7. N.K. Dhar, P.R. Boyd, M. Martinka, J.H. Dinan, L.A. Almeida, and N. Goldsman, *J. Electron. Mater.* 29, 748 (2000).
8. N.K. Dhar, N. Goldsman, and C.E.C. Wood, *Phys. Rev. B* 61, 8256 (2000).
9. C. Fulk, R. Sporken, J. Dumont, D. Zavitz, M. Trenary, B. Gupta, G. Brill, J. Dinan, and S. Sivananthan, *J. Electron. Mater.* 34, 846 (2005).
10. M. Carmody, S. Mallick, J. Margetis, R. Kodama, T. Biegala, D. Xu, P. Bechmann, J.W. Garland, and S. Sivananthan, *Appl. Phys. Lett.* 96, 153502 (2010).
11. A. Ishizaka and Y. Shiraki, *J. Electrochem. Soc.* 133, 666 (1986).
12. D. Hull and D.J. Bacon, *Introduction to Dislocations* (Woburn: Butterworth Heinemann, 2001).
13. D.J. Smith, S.C.Y. Tsen, D. Chandrasekhar, P.A. Crozier, S. Rujirawat, G. Brill, Y.P. Chen, R. Sporken, and S. Sivananthan, *Mater. Sci. Eng. B* 77, 93 (2000).
14. S. Rujirawat, L.A. Almeida, Y.P. Chen, S. Sivananthan, and D.J. Smith, *Appl. Phys. Lett.* 71, 1810 (1997).
15. S.H. Shin, J. Bajaj, L.A. Moudy, and D.T. Cheung, *Appl. Phys. Lett.* 43, 68 (1983).
16. N.G. Chew, A.G. Cullis, and G.M. Williams, *Appl. Phys. Lett.* 45, 1090 (1984).
17. T. Aoki, Y. Chang, G. Badano, J. Zhao, C. Grein, S. Sivananthan, and D.J. Smith, *J. Cryst. Growth* 265, 224 (2004).